Physics and Imaging in Radiation Oncology 32 (2024) 100649

Contents lists available at ScienceDirect

Physics and Imaging in Radiation Oncology

journal homepage: www.sciencedirect.com/journal/physics-and-imaging-in-radiation-oncology

Original Research Article

Machine learning automated treatment planning for online magnetic resonance guided adaptive radiotherapy of prostate cancer

Aly Khalifa [a,b], Jeff D. Winter [c,d,e], Tony Tadic [c,d,e], Thomas G. Purdie [a,c,d,e,*], Chris McIntosh [a,b,f,g,h,i,j,**]

[a] Department of Medical Biophysics, University of Toronto, Toronto, Ontario, Canada
[b] Toronto General Hospital Research Institute, University Health Network, Toronto, Ontario, Canada
[c] Medical Physics, Princess Margaret Cancer Centre, Toronto, Ontario, Canada
[d] Department of Radiation Oncology, University of Toronto, Toronto, Ontario, Canada
[e] Princess Margaret Cancer Research Institute, University Health Network, Toronto, Ontario, Canada
[f] Peter Munk Cardiac Centre and Ted Rogers Centre for Heart Research, University Health Network, Toronto, Ontario, Canada
[g] Department of Computer Science, University of Toronto, Toronto, Ontario, Canada
[h] Joint Department of Medical Imaging, University Health Network, Toronto, Ontario, Canada
[i] Department of Medical Imaging, University of Toronto, Toronto, Ontario, Canada
[j] Vector Institute, Toronto, Ontario, Canada

ARTICLE INFO

Keywords:
Automation
Treatment planning
Adaptive radiotherapy
Prostate cancer
Machine learning
Artificial intelligence

ABSTRACT

Background and purpose: No best practices currently exist for achieving high quality radiation therapy (RT) treatment plan adaptation during magnetic resonance (MR) guided RT of prostate cancer. This study validates the use of machine learning (ML) automated RT treatment plan adaptation and benchmarks it against current clinical RT plan adaptation methods.

Materials and methods: We trained an atlas-based ML automated treatment planning model using reference MR RT treatment plans (42.7 Gy in 7 fractions) from 46 patients with prostate cancer previously treated at our institution. For a held-out test set of 38 patients, retrospectively generated ML RT plans were compared to clinical human-generated adaptive RT plans for all 266 fractions. Differences in dose-volume metrics and clinical objective pass rates were evaluated using Wilcoxon tests ($p < 0.05$) and Exact McNemar tests ($p < 0.05$), respectively.

Results: Compared to clinical RT plans, ML RT plans significantly increased sparing and objective pass rates of the rectum, bladder, and left femur. The mean ± standard deviation of rectum D20 and D50 in ML RT plans were 2.5 ± 2.2 Gy and 1.6 ± 1.3 Gy lower than clinical RT plans, respectively, with 14 % higher pass rates; bladder D40 was 4.6 ± 2.9 Gy lower with a 20 % higher pass rate; and the left femur D5 was 0.8 ± 1.8 Gy lower with a 7 % higher pass rate.

Conclusions: ML automated RT treatment plan adaptation increases robustness to interfractional anatomical changes compared to current clinical adaptive RT practices by increasing compliance to treatment objectives.

1. Introduction

In recent years, advances in magnetic resonance (MR) guided adaptive radiotherapy (RT) have significantly increased the precision of prostate RT. By leveraging the high soft-tissue contrast of MR, RT treatment plans can be safely adapted during every fraction (i.e. online) to daily changes in the position or shape of organs-at-risk (OAR), such as the rectum and bladder, and target volumes [1–3] to improve adherence to treatment objectives [4,5]. Additionally, MR imaging has the potential to reduce acute toxicity in prostate RT by enabling reduced treatment margins compared to other imaging modalities [6]. However, the increased workflow complexity and human resource burden of online adaptive RT has hindered its implementation and adoption as a routine RT option [7].

* Corresponding author at: Department of Radiation Oncology, University of Toronto, 149 College St., Toronto ON M5T 1P5, Canada.
** Corresponding author at: Department of Medical Biophysics, University of Toronto, 101 College St., Toronto ON M5G 1L7, Canada.
E-mail addresses: aly.khalifa@mail.utoronto.ca (A. Khalifa), tom.purdie@uhn.ca (T.G. Purdie), chris.mcintosh@uhn.ca (C. McIntosh).

https://doi.org/10.1016/j.phro.2024.100649
Received 1 August 2024; Received in revised form 3 September 2024; Accepted 11 September 2024
Available online 14 September 2024

There are currently no universally accepted best-practices for achieving high quality online adaptive RT plans. Standard inverse planning techniques are not suitable for the time constraints required for online RT plan adaptation. Instead, available methods rely on iterative re-optimization of a reference plan to suit daily anatomy, creating a trade-off between time spent RT plan adaptation with the overall treatment time [5]. Consequently, current RT plan adaptation methods may not maximize the achievable RT plan quality [8,9], causing institutions to instead rely on methods of increasing set-up consistency, such as rectal balloons [10], to reduce the need for RT plan adaptation. These challenges underscore the need for more robust and efficient RT plan adaptation approaches.

This paper investigates the application of machine learning (ML) automated RT treatment planning, introduced by McIntosh et al. [11], as an RT plan adaptation strategy. We benchmark it against the current RT plan adaptation method in clinical use at our institution for adaptive treatment of prostate cancer. While other automated approaches have been proposed in the literature [8,9], our proposed method leverages ML dose predictions to tailor RT plans to daily patient anatomy, which are then transformed to a deliverable RT plan using a dose mimicking algorithm [11]. This method has been shown to reduce treatment planning times and increase standardization of RT plan quality in the non-adaptive RT setting [12]. We therefore hypothesise that ML will increase robustness to inter-fractional anatomical variation to provide an efficient and accurate online RT plan adaptation strategy.

2. Materials and methods

2.1. Data collection

RT imaging and treatment planning data was collected from 84 patients with intermediate risk prostate cancer treated on a 1.5 T MR-linear accelerator (Unity, Elekta, Stockholm, Sweden) between August 2020 and August 2023. All patients were prescribed a dose of 42.7 Gy in 7 fractions to the whole prostate gland. RT plans used 7 MV-FFF photon beams with a standard 9-beam arrangement at pre-defined gantry angles (0°, 35°, 65°, 95°, 145°, 215°, 265°, 295°, and 325° delivered using step-and-shoot intensity modulated RT. Patients were treated as part of two clinical trials on MR-guided RT approved by our institutional Research Ethics Review Board. Further ethics approval of this study was waived as part of an ongoing quality improvement initiative for automated ML treatment planning. Patients were further divided into a training dataset (n = 46) if they were treated before October 20, 2022 and remaining patients were assigned to a testing dataset (n = 38). The training dataset was used to train the ML model, as described below, while the testing dataset was used for comparing the ML and clinical adaptive RT treatment planning approaches. This dataset splitting approach was selected to provide a realistic assessment of ML performance using standard deployment practices, where training data is first accrued as patients are treated and then the trained ML is deployed into the clinic for validation and treatment.

2.2. Clinical RT treatment workflow

All patients undergo MR simulation imaging on the MR-linear accelerator with an empty rectum and comfortably full bladder, achieved by having patients empty their bladder and drink 300 mL of water 15 min before simulation. The planning MR is the vendor-provided 3D T2-weighted MR scan. A radiation oncologist contours the prostate clinical target volume (CTV), whole bladder, rectum, urethra, penile bulb, as well as the small and large bowels if proximal to the CTV. A RT planner (dosimetrist) contours the femurs. The planning target volume (PTV) is a 4 mm expansion of the CTV with 3 mm margins in left–right direction. A standard CT simulation scan is used to extract mean electron density values for the PTV, femurs, and external contours, which are applied as density overrides on the reference MR image for dose calculation.

Reference RT treatment planning is then performed in the MR-linear accelerator RT treatment planning system (Monaco 5.4 or 5.51, Elekta, Stockholm, Sweden) using a standard optimization objectives template that is modified as required by the RT planner. Dose calculation is performed with Monaco Monte Carlo which accounts for the MR B-field. The RT plan then undergoes standard radiation oncology and medical physics review and patient-specific quality assurance measurements.

During each treatment fraction, a new adapted RT plan is generated based on the contours and optimization objectives from the MR reference RT plan. The adaptive RT treatment protocol begins with acquisition of a localization T2-weighted 3D MR image for adaptive RT planning. Following an initial soft-tissue rigid registration of the reference and localization MR images, contours are mapped to the localization image using deformable image registration. The mapped contours are manually edited by a radiation oncology fellow or RT planner as needed.

Finally, the adapted RT plan is generated by re-optimization of the segment weights and shapes from fluence, using the optimization objectives of the reference RT plan as a starting point. During the optimization process, RT planners modify optimization objectives as needed to improve plan quality and meet the dose-volume histogram (DVH) clinical objectives (Table 1). This optimization process takes an average of 5.4 min (for patients in the test set). At the end of optimization, verification imaging is performed to check for intra-fractional motion. If motion is deemed significant, the optimized plan is rigidly registered to the verification image. The adapted RT plan then undergoes online plan quality assurance and is delivered.

2.3. Machine learning RT treatment plans

We generated ML adapted RT plans using the atlas-based ML dose prediction method introduced by McIntosh et al. for automated treatment planning in a commercial RT treatment planning system (RayStation 8B, RaySearch, Stockholm, Sweden) [11,13]. The method uses an ML model to select RT plans from the training set (referred to as atlases) that are suitable to the anatomy of the patient. Information from the atlases is used to predict clinically desirable voxel-wise dose distributions for the new RT plan, which is converted to deliverable RT plan using a dose-mimicking algorithm. ML RT plan creation takes approximately 12–13 min without human interaction when run using a limited performance research server [11].

A MR-specific ML model was trained using only the pre-treatment reference RT plans of the patients in the training set to ensure that the model learned from RT plans that had gone through rigorous manual optimization iterations and that their dose distributions were best for the reference plan anatomy. Additionally, the use of MR simulation RT plans ensures that the model learns MR-specific features to avoid issues with ML domain shift [14].

The trained ML model was then used to retrospectively generate RT plans for each treatment fraction in the test set, described above, to simulate ML RT plan adaptation at each fraction, using the same contours and density overrides as those used for creating clinical adapted RT plans. RT dose-mimicking was configured to use a clinical beam model for the MR-linear accelerator, using the collapsed cone dose calculation engine in RayStation. Although a different dose calculation engine from clinical RT planning was used, the use of central targets with uniform density overrides on the PTV, external, and femurs limits potential impact of dose calculation algorithm differences between the RayStation and Monaco RT treatment planning systems. Additionally, the ML model was trained on distributions generated using the Monaco dose calculation engine, with the dose-mimicking step designed to recreate the ML predicted dose. The closest possible settings for fluence segmentation as those used for generating the clinical RT plan in Monaco were used. Note that unlike the clinical adaptive RT treatment planning method described above, the ML RT plans generated at each fraction have no

Table 1
Mean DVH metrics and pass rates for ML and clinical RT plans for all 266 treatment fractions included in the test set, evaluated using our institutional protocol. Negative dose differences and pass rates indicate a lower ML RT plan dose and pass rate, respectively. Bolded text indicates statistically significant differences in DVH metrics (Wilcoxon tests; $p < 0.05$) or pass rates (McNemar tests; $p < 0.05$). SD = standard deviation.

Region of interest	Objective (Gy)	Mean dose ± SD (Gy)			Pass rate (%)		
		ML	Clinical	Difference	ML	Clinical	Difference
CTV	D99 > 42.7	43.3 ± 0.3	42.8 ± 0.2	**0.5 ± 0.3**	100.0	100.0	0
PTV	D99 > 40.6	40.8 ± 0.2	40.7 ± 0.1	**0.1 ± 0.2**	100.0	100.0	0
	D1cc < 46.1	44.7 ± 0.4	45.1 ± 0.3	**−0.4 ± 0.4**	99.2	98.1	1.1
Rectum	D20 < 24.0	17.2 ± 3.4	19.7 ± 4.6	**−2.5 ± 2.2**	97.0	83.1	**13.9**
	D50 < 10.0	6.7 ± 1.3	8.2 ± 1.8	**−1.6 ± 1.3**	99.6	85.3	**14.3**
	D1cc < 42.7	38.8 ± 6.2	39.0 ± 6.1	**−0.2 ± 0.9**	78.6	76.7	1.9
Bladder	D40 < 18.0	12.1 ± 7.2	16.8 ± 6.8	**−4.6 ± 2.9**	77.4	57.1	**20.3**
	D5cc < 42.7	37.9 ± 4.5	39.7 ± 2.8	**−1.8 ± 2.2**	96.6	97.4	−0.8
Small Bowel	D1cc < 30	4.8 ± 6.5	6.9 ± 8.3	**−2.0 ± 2.6**	99.5	100.0	−0.5
Large Bowel	D1cc < 30	2.8 ± 3.5	4.6 ± 5.2	**−1.8 ± 2.3**	100.0	99.6	0.4
Penile Bulb	D1cc < 42.7	5.7 ± 5.7	9.8 ± 8.6	**−4.1 ± 3.9**	100.0	100.0	0
	D50 < 34.2	2.7 ± 1.1	4.7 ± 3.2	**−1.9 ± 2.2**	100.0	100.0	0
Left Femur	D5 < 18.0	15.7 ± 1.3	16.5 ± 1.4	**−0.8 ± 1.8**	98.1	91.0	**7.1**
Right Femur	D5 < 18.0	15.7 ± 1.4	16.3 ± 1.2	**−0.6 ± 1.8**	97.4	93.2	4.2
Urethra	D50 < 45.0	44.0 ± 0.3	44.0 ± 0.3	**0.1 ± 0.4**	98.9	99.6	−0.7

dependence on the reference RT plan.

2.4. ML vs. clinical RT plan comparison

ML and clinical adapted RT plans were evaluated using our institutional plan evaluation protocol, which specifies DVH metrics and planning objectives (Table 1). Differences in DVH metrics between ML and clinical RT plans were assessed using paired two-sided Wilcoxon Signed Rank tests. Differences in the rates at which plans met protocol limits were assessed using Exact McNemar's tests. False discovery rate correction was applied to all comparisons to control the type II error rate [15], using a significance threshold of 5 % ($p < 0.05$). Statistical testing was performed using the SciPy version 1.11.1 [16] and statsmodels version 0.14.0 [17] Python packages.

2.5. Plan indexes and machine parameters

The spatial dose distributions of ML and clinical RT plans were compared using the conformity index (CI) and homogeneity index (HI). The CI was calculated as the ratio of the PTV volume covered by the 4060 cGy isodose line (95 % of prescription) to the total isodose volume. The HI was calculated as the ratio of PTV D5 to PTV D95. Finally, machine parameters were compared using the total number of MLC segments and monitor units (MU) per fraction. All indexes and parameters were calculated in the RayStation treatment planning system.

3. Results

3.1. DVH metrics

We found that ML RT plan adaptation increased sparing for several OAR, bringing several RT plans within acceptance limits where the clinical method could not. As shown in Table 1, all differences in mean DVH metrics were statistically significant ($p < 0.05$), indicating sufficient study power to detect even small dose differences, although they may not be clinically significant. Only a subset of DVH metric differences were associated with significant differences in clinical objective pass rates: the mean ± the standard deviation of rectum D20 and D50 in ML RT plans were 2.5 ± 2.2 Gy and 1.6 ± 1.3 Gy lower than that of clinical RT plans, respectively, resulting in a 13.9 % and 14.3 higher pass rate; bladder D40 was 4.6 ± 2.9 Gy lower with a 20.3 % higher pass rate; and finally, the left femur D5 was 0.8 ± 1.8 Gy lower with a 7.1 % higher pass rate. However, ML RT plan adaptation did not lower the mean dose for all OAR. ML RT plans produced a slightly higher urethra dose (+0.06 Gy) and fewer ML RT plans passed the objectives for bladder D5cc and small bowel D1cc despite having a lower mean dose.

The average ML and clinical DVH curves and the distribution of DVH metrics differences for the target structures (CTV and PTV), bladder, and rectum for every fraction in the test set are shown in Fig. 1. The DVH curves demonstrate that the increased sparing by ML is observed throughout the entire OAR volume and not just at the specific points evaluated in the protocol. Although the ML increases OAR sparing on average, ML RT plans occasionally produce higher OAR doses than clinical RT plans. This scenario likely only occurs when the achievable dose range at a particular fraction is well below the OAR limit, given the higher pass rates of ML RT plans. The exception was for absolute volume criteria (PTV D1cc, bladder D5cc, and rectum D1cc), where the ML RT plans had higher doses in up to 50 % of cases, suggesting that hotspots are more common in ML RT plans. The largest dose differences between ML and clinical RT plans were associated with large transient anatomical changes, as exemplified in Fig. 2. For this patient, changes in rectum and bladder fullness heavily influenced the OAR sparing achievable by either planning method. However, the ML RT plan was more robust to these anatomical changes and achieved the clinical goal.

3.2. Plan indexes and machine parameters

The average CI, HI, total MU per fraction, and the total number of segments are reported in Table 2. ML and clinical RT plans had similar dose homogeneity and conformity, with average CI and HI values of 0.82 to 0.83 and 1.03 to 1.04, respectively. Both plan types had similar ranges of total MU per fraction of 1414 to 1455 MU. However, clinical RT plans were more modulated, using an average of 68.8 segments compared to 49.6 segments for ML RT plans. This discrepancy is likely a result of the different fluence map optimization algorithms used by the RayStation and Monaco RT treatment planning systems.

4. Discussion

Automated treatment planning has the potential to standardize and accelerate adaptive RT by accurately predicting the best achievable daily dose and reducing the need for human interaction during the planning process. In this study, both ML and clinical adaptive RT methods were effective in meeting the treatment objectives of our clinical protocol. However, the ML RT plan adaptation method was more robust to interfractional anatomical changes, benefitting patients with unfavourable anatomy the most. For example, in cases where neither adaptation method achieved clinical objectives, the ML method increased sparing beyond what was achieved in the clinical plan. There were also cases in which only the ML RT plan was able to achieve the

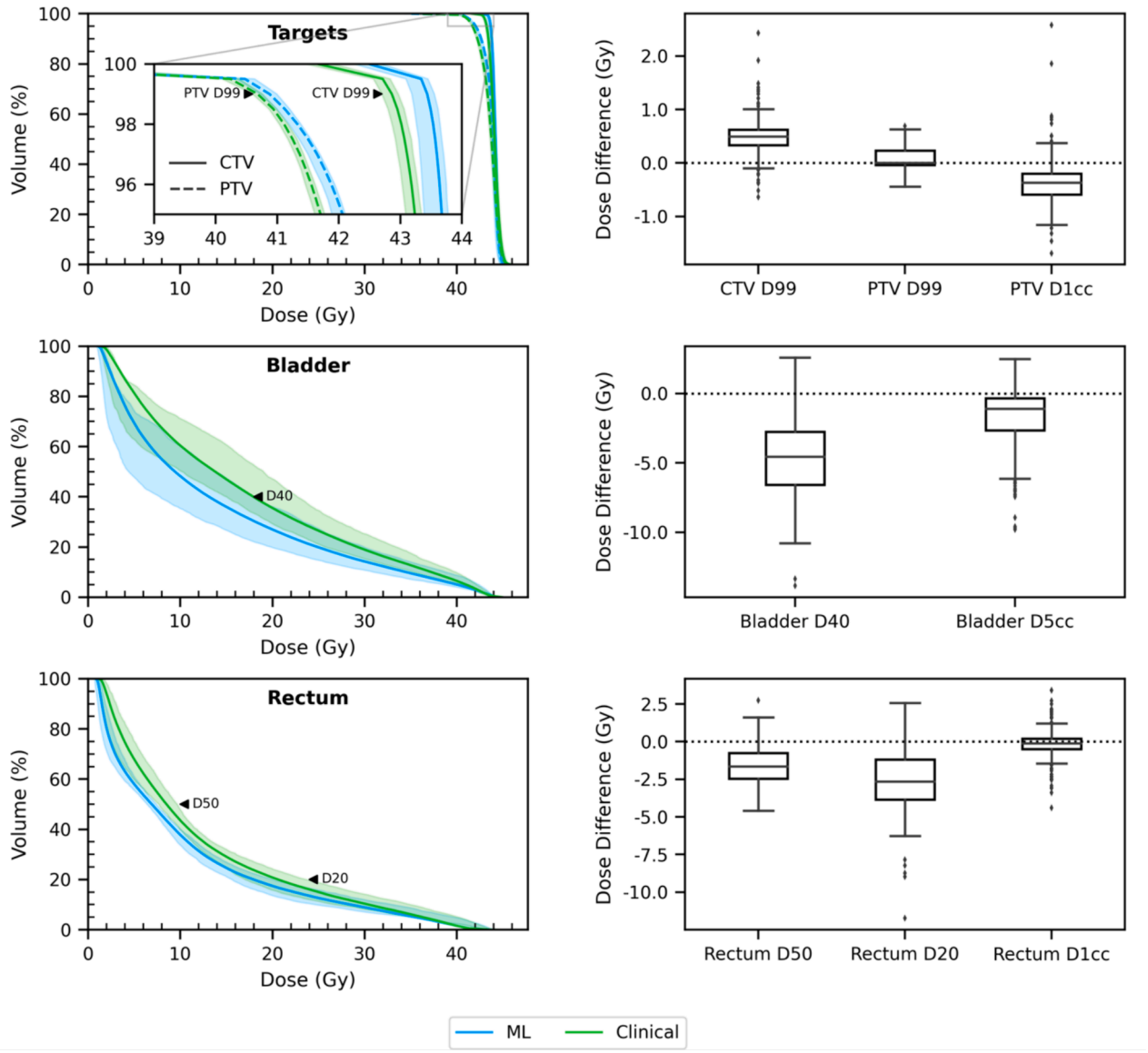

Fig. 1. Left: Average DVH of ML and Clinical RT plans in the test set, with error bars indicating the interquartile range. Upper (bladder and rectum) and lower (targets) dose objectives are indicated by black arrows, where DX indicates the dose received by X% of the ROI volume. Right: Differences in clinical DVH metrics between ML and clinical RT plans, where negative values indicate a lower ML RT plan dose. Outliers are defined as points greater than 1.5 times the interquartile range away from the median.

clinical objectives.

The reduced robustness of the clinical RT plan adaptation method is likely due to the unique planning challenges in the online setting. In the clinical method, RT plan adaptation is constrained by reference optimization objectives that may not generalize well to daily anatomy, resulting in suboptimal adapted RT plans. In these instances, RT planners may refine the plan but at the expense of extending the treatment time. Therefore, they may choose to limit the time spent on adaptation and sacrifice potential improvements in OAR sparing.

In contrast, the ML method is robust to interfractional anatomical changes as it treats each fraction independently by tailoring dose predictions to daily anatomy. This eliminates the need for iterative fine-tuning of the adapted RT plan and reduces the dependence on human planners during treatment. Therefore, ML planning has the potential to ease the current resource demands of adaptive RT, which typically requires a large, specialized team to oversee and execute plan adaptation [7]. Instead, expertise would be needed in upstream development processes, such as data curation and ML model training. However, a limitation of the method is the time needed to curate a sufficiently large dataset for ML training, which could be a challenge for newer or rarer treatments.

Our findings align with recent studies that integrate automated treatment planning methods into MR-guided prostate adaptive RT, such as mCycle [9] and Particle Swarm Optimization (PSO) [8]. mCycle uses lexographic optimization based on a user-specified “wish-list” of optimization objectives and constraints, whereas PSO selects plans with the highest quality score from a solution space of possible plans. Both methods reduce human interaction in the RT plan adaptation process but still rely on optimization objectives, unlike the ML approach, which is data-driven and learns desirable RT plans from the training dataset. Despite these technical differences, these studies also found improvements in OAR sparing were possible compared to clinical adaptive RT methods, especially for large anatomical changes. However, the specific benefits varied. For example, mCycle improved rectum sparing but not bladder sparing, in contrast to our finding, which showed large improvements in bladder sparing. These discrepancies are likely the result of both the small patient cohorts studied and the diversity of treatment planning and evaluation protocols used. Larger multicenter studies are

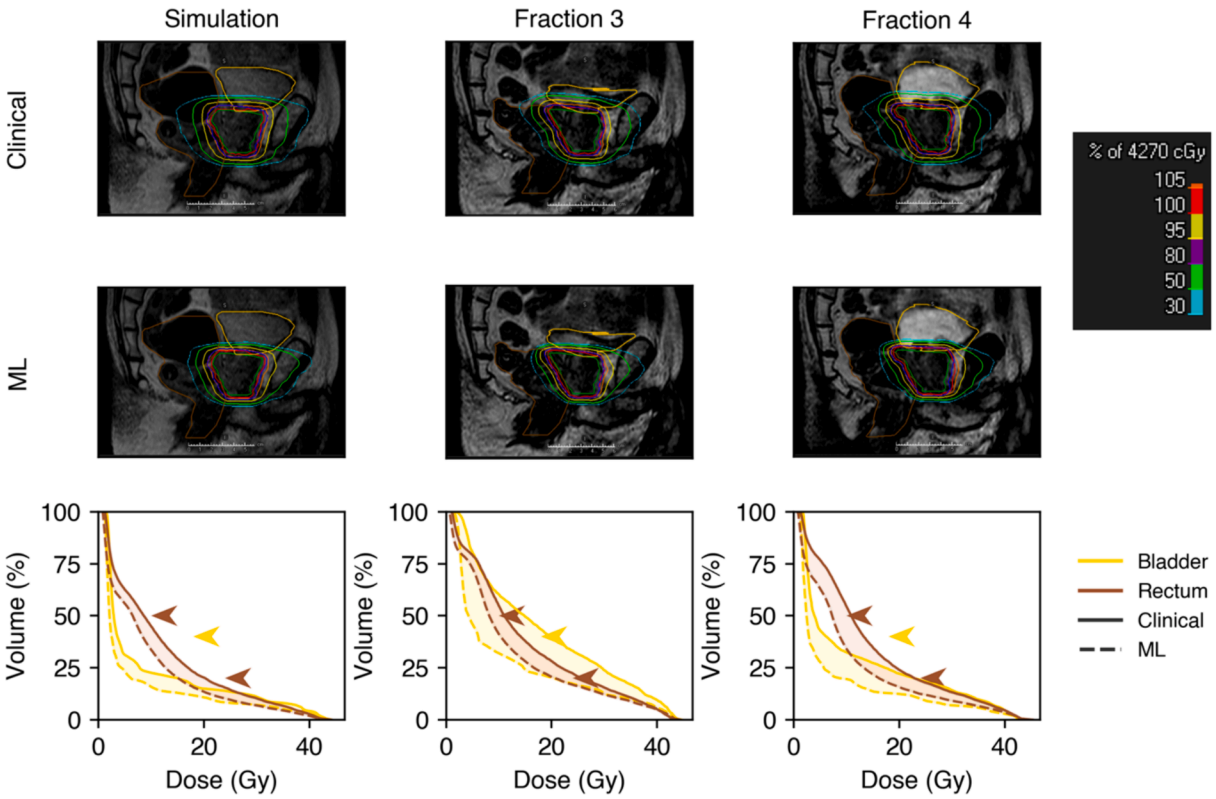

Fig. 2. A patient case demonstrating how achievable DVH curves between ML (dashed line) and clinical (solid line) RT plan adaptation methods corresponds with anatomical variation between fractions, such as rectum and bladder fullness. The contours shown are the CTV (green), PTV (blue), bladder (yellow), and rectum (brown). Arrows indicate institutional planning objectives, color-coded to the organ. (For interpretation of the references to color in this figure legend, the reader is referred to the web version of this article.)

Table 2
Comparison of mean plan parameters ± the standard deviation between ML and clinical RT treatment planning methods.

Planning method	Conformity Index (CI)	Homogeneity Index (HI)	Total MU/ fraction	Total MLC segments/ fraction
ML	0.828 ± 0.023	1.026 ± 0.002	1414.5 ± 119.7	49.6 ± 0.7
Clinical	0.824 ± 0.036	1.040 ± 0.003	1455.4 ± 111.4	68.8 ± 3.2

needed to make these results more widely applicable.

To be clinically feasible, automated techniques must also be sufficiently fast to be compatible with online adaptive RT. In our study, the optimization time for the ML method using a limited performance research server was 12–13 min [11], which was twice the optimization time of the clinical workflow (5.4 min on average). However, the ML optimization can be accelerated in the future with improved hardware and parallelization of the dose mimicking. In comparison, mCycle reported an optimization time of 8 min [9], whereas PSO requires up to two hours to generate an RT plan [8]. Future work should focus on accelerating the optimization time of these techniques.

A limitation of this study is its retrospective nature, which only simulates ML performance in a research setting. In real clinical settings, clinicians' assessment of ML performance is influenced by human factors such as subjective preference towards nuanced plan features or confidence in the safety of ML tools [12]. To address this, integrating the automation into existing adaptive RT treatment and quality assurance protocols is needed. This would allow clinicians to gain hands-on experience with ML-automated RT plan adaptation and assess its efficacy and compatibility with existing treatment workflows. Unfortunately, prospective deployment of our method is currently limited by the closed nature of the MR linear accelerator's treatment planning system, which does not currently support the use of externally generated RT plans during online treatment.

In summary, our study demonstrates that ML automated RT plan adaptation increases compliance with treatment protocols and robustness to interfractional anatomical changes compared to current clinical adaptive RT practices in the context of prostate RT. Critically, our work shows that current online RT plan adaptation methods in clinical use do not maximize adaptive RT plan quality, potentially limiting the clinical benefits of adaptation. As ongoing international efforts continue to establish the clinical benefits of online MR-guided RT [18], it is crucial to employ the best treatment planning tools to achieve meaningful clinical outcomes.

CRediT authorship contribution statement

Aly Khalifa: Conceptualization, Data curation, Formal analysis, Investigation, Methodology, Project administration, Visualization, Writing – original draft. **Jeff D. Winter:** Conceptualization, Data curation, Supervision, Writing – review & editing. **Tony Tadic:** Data curation. **Thomas G. Purdie:** Conceptualization, Methodology, Resources, Supervision, Writing – review & editing. **Chris McIntosh:** Conceptualization, Methodology, Resources, Supervision, Writing – review & editing.

Declaration of competing interest

The authors declare the following financial interests/personal relationships which may be considered as potential competing interests: The authors declare the following financial interests/personal

relationships which may be considered as potential competing interests: Thomas G Purdie and Chris McIntosh receive royalties from RaySearch Laboratories for machine-learning based treatment planning methods.

Acknowledgments

This study is supported by Canadian Institute of Health Research (CIHR) Grant PJT-183757, Natural Science and Engineering Research Council of Canada (NSERC) Grant RGPIN-2022-04163, and Princess Margaret Cancer Foundation (PMCF) grants.

References

[1] Bruynzeel AME, Tetar SU, Oei SS, Senan S, Haasbeek CJA, Spoelstra FOB, et al. A prospective single-arm phase 2 study of stereotactic magnetic resonance guided adaptive radiation therapy for prostate cancer: early toxicity results. Int J Radiat Oncol Biology Phys 2019;105:1086–94. https://doi.org/10.1016/j.ijrobp.2019.08.007.

[2] Teunissen FR, Willigenburg T, Tree AC, Hall WA, Choi SL, Choudhury A, et al. Magnetic resonance-guided adaptive radiation therapy for prostate cancer: the first results from the MOMENTUM STUDY—An international registry for the evidence-based introduction of magnetic resonance-guided adaptive radiation therapy. Pract Radiat Oncol 2023;13:e261–9. https://doi.org/10.1016/j.prro.2022.09.007.

[3] Sritharan K, Daamen L, Pathmanathan A, Schytte T, Pos F, Choudhury A, et al. MRI-guided radiotherapy in twenty fractions for localised prostate cancer; results from the MOMENTUM study. Clin Transl Radiat Oncol 2024:100742. https://doi.org/10.1016/j.ctro.2024.100742.

[4] Alexander SE, McNair HA, Oelfke U, Huddart R, Murray J, Pathmanathan A, et al. Prostate volume changes during extreme and moderately hypofractionated magnetic resonance image-guided radiotherapy. Clin Oncol 2022. https://doi.org/10.1016/j.clon.2022.03.022.

[5] Winkel D, Bol GH, Kroon PS, van Asselen B, Hackett SS, Werensteijn-Honingh AM, et al. Adaptive radiotherapy: the Elekta Unity MR-linac concept. Clin Transl Radiat Oncol 2019;18:54–9. https://doi.org/10.1016/j.ctro.2019.04.001.

[6] Kishan AU, Ma TM, Lamb JM, Casado M, Wilhalme H, Low DA, et al. Magnetic resonance imaging-guided vs computed tomography-guided stereotactic body radiotherapy for prostate cancer. JAMA Oncol 2023:9. https://doi.org/10.1001/jamaoncol.2022.6558.

[7] Bertholet J, Anastasi G, Noble D, Bel A, van Leeuwen R, Roggen T, et al. Patterns of practice for adaptive and real-time radiation therapy (POP-ART RT) part II: offline and online plan adaption for interfractional changes. Radiother Oncol 2020. https://doi.org/10.1016/j.radonc.2020.06.017.

[8] Tengler B, Künzel LA, Hagmüller M, Mönnich D, Boeke S, Wegener D, et al. Full daily re-optimization improves plan quality during online adaptive radiotherapy. Phys Imaging Radiat Oncol 2024;29:100534. https://doi.org/10.1016/j.phro.2024.100534.

[9] Naccarato RS, Pellegrini M, Voet R, Akhiat P, Gurrera H, et al. Automated planning for prostate stereotactic body radiation therapy on the 1.5 T MR-Linac. Adv Radiat Oncol 2022:7. https://doi.org/10.1016/j.adro.2021.100865.

[10] Poon DMC, Yang B, Geng H, Wong OL, Chiu ST, Cheung KY, et al. Analysis of online plan adaptation for 1.5T magnetic resonance-guided stereotactic body radiotherapy (MRgSBRT) of prostate cancer. J Cancer Res Clin Oncol 2023;149:841–50. https://doi.org/10.1007/s00432-022-03950-1.

[11] McIntosh C, Welch M, McNiven A, Jaffray DA, Purdie TG. Fully automated treatment planning for head and neck radiotherapy using a voxel-based dose prediction and dose mimicking method. Phys Med Biol 2017;62:5926–44. https://doi.org/10.1088/1361-6560/aa71f8.

[12] McIntosh C, Conroy L, Tjong MC, Craig T, Bayley A, Catton C, et al. Clinical integration of machine learning for curative-intent radiation treatment of patients with prostate cancer. Nat Med 2021:1–7. https://doi.org/10.1038/s41591-021-01359-w.

[13] McIntosh C, Purdie TG. Contextual atlas regression forests: multiple-atlas-based automated dose prediction in radiation therapy. IEEE Trans Med Imaging 2016;35:1000–12. https://doi.org/10.1109/tmi.2015.2505188.

[14] Khalifa A, Winter JD, Navarro I, McIntosh C, Purdie TG. Domain adaptation of automated treatment planning from computed tomography to magnetic resonance. Phys Med Biol 2022. https://doi.org/10.1088/1361-6560/ac72ec.

[15] Benjamini Y, Hochberg Y. Controlling the false discovery rate: a practical and powerful approach to multiple testing. J R Stat Soc Series B Stat Methodol 1995;57:289–300.

[16] Virtanen P, Gommers R, Oliphant TE, Haberland M, Reddy T, Cournapeau D, et al. SciPy 1.0: fundamental algorithms for scientific computing in Python. Nat Methods 2020;17:261–72. https://doi.org/10.1038/s41592-019-0686-2.

[17] Seabold S, Perktold J. statsmodels: Econometric and statistical modeling with python. 9th Python in Science Conference, 2010.

[18] van Otterloo SR de M, Christodouleas JP, Blezer ELA, Akhiat H, Brown K, Choudhury A, et al. Patterns of care, tolerability, and safety of the first cohort of patients treated on a novel high-field MR-Linac within the MOMENTUM study: initial results from a prospective multi-institutional registry. Int J Radiat Oncol Biol Phys 2021;111:867–75. https://doi.org/10.1016/j.ijrobp.2021.07.003.